

SYNTHESIS, CHARACTERIZATION AND PREDICTION OF ANTICANCER POTENTIALITY OF SOME NOVEL GREEN NANOPARTICLES BY MOLECULAR DOCKING AND ADMET TECHNIQUES

Savita Belwal^{1*}, R. Saritha¹, Harshita Sachdeva² and Gangarapu Kiran³

¹Department of Chemistry, Anurag Group of Institutions, Hyderabad, Telangana, India

²Department of Chemistry, University of Rajasthan, Jaipur-302004, India

³Department of Pharmacy, Anurag Group of Institutions, Hyderabad, Telangana, India

(Received August 1, 2019; Revised August 13, 2019; Accepted August 16, 2019)

ABSTRACT. Anticancer potentiality of some newly synthesized Nano-Biginelli compounds with the help of enzyme extracted naturally from plants is reported. The biological synthesis of nanoparticles via nano biotechnology processes have a significant potential to enhance the production without the use of harsh, toxic, and expensive chemicals commonly used in conventional physical and chemical processes. The compounds have been characterized on the basis of UV, FTIR, XRD and SEM studies in order to depict the formation of nanoparticles. Using the combination of docking and ADMET techniques, we have tried to predict the anti-cancer potentiality as well as its area of target, i.e. cancer cell to trigger the anti-cancer reaction. Results indicate that the compound **1** (ethyl-6-methyl-2-oxo-4-(4-methoxyphenyl)-1,2,3,4-tetrahydropyrimidin-5-carboxylate) has possible virtual leads to design novel human *Aurora B kinase* inhibitor.

KEY WORDS: Nano biotechnology, Green chemistry, Enzymes, Drug research

INTRODUCTION

Nanotechnology is the creation, manipulation and use of materials at the nanometer size scale (1 to 100 nm). There is a tremendous growth in the field of nano science and nanotechnology over the past two decades. Nanomaterials have numerous applications in the field of electronics, cosmetics, coatings, packaging and biotechnology [1]. There are several reports in the literature [2-6] which show an amazing level of their performance as catalysts in terms of selectivity, reactivity and improved yields of products.

In addition, the high surface-to-volume ratio of nanoparticles provides a larger number of active sites per unit area compared to their heterogeneous counterparts. Catalysis by transition metal nanoparticle has undergone an explosive growth during the past decade [7]. Recyclability is one of the most important properties of nanoparticles which make chemical synthesis ecofriendly green protocol. Nano catalyst can be easily reused and recycled for numerous cycles with unswerving activity.

Even though metal nanoparticles are being increasingly used in many segments of the economy, there is growing interest in the biological and environmental safety of their production. The main methods for nanoparticle production are chemical and physical approaches that are often costly and potentially detrimental to the environment. Thus, there is a great need for an alternative, cost-effective and at the same time safe and environmentally sound method of nanoparticle production. Although nanoparticles can be synthesized by various traditional methods, it is now possible to biologically synthesize these materials via environment-friendly green chemistry based techniques.

In recent years, the convergence between nanotechnology and biology has created the new field of nano biotechnology that incorporates the use of biological entities such as actinomycetes [8], algae, bacteria [9], fungi [10], viruses [11], yeasts, and plants [12] in a number of

*Corresponding author. E-mail: saovita29@gmail.com

This work is licensed under the Creative Commons Attribution 4.0 International License

biochemical and biophysical processes. To improve nanoparticles production without the use of harsh, toxic, and expensive chemicals commonly used in conventional physical and chemical processes, currently biological synthesis via nano biotechnology has been used [13]. Biosynthesis of nanoparticles by means of plants or plant based extracts tends to be safe, have relatively short production times, and a lower fabrication cost compared to other biological systems.

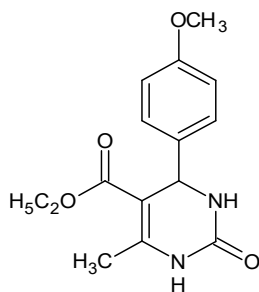
Among heterocyclic compounds, 3,4-dihydropyrimidinones (Biginelli compounds) [14] are highly contained in organic synthesis due to their attractive pharmacological properties, including calcium channel blockers, antihypertensive agents, α -1a-antagonists, HIV gp-120-CD4 inhibitors (crambine and betzellidine alkaloids), antiviral, antitumour, antibacterial activities and neuropeptide Y(NPY) antagonists.

Hence, in continuation to our interest on the synthesis of heterocyclic compounds by green protocols and provoked by the diverse biological activities associated with Biginelli compounds, we now synthesize some novel Nano-Biginelli compounds with the help of enzyme extracted naturally from the plant. Compounds have been characterized on the basis of UV, FTIR, XRD and SEM in order to depict the formation of nanoparticles and determination of their size and shape.

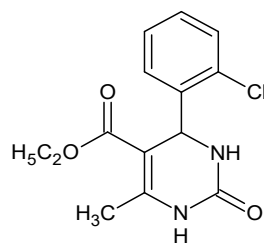
EXPERIMENTAL

Reagents and solvents were purchased from commercial sources and used without further purification. Melting points were determined on a Toshniwal apparatus. The purity of compounds was checked on thin layers of silica gel in various non-aqueous solvent systems, e.g. benzene : ethyl acetate (9:1), benzene : ethyl acetate : methanol (8.5:1.4:0.1). UV-Visible spectra were recorded on UV1800S, Shimadzu, Japan. IR spectra of the synthesized compounds **1** and **2** were recorded in KBr on a Perkin Elmer Infrared RXI FTIR spectrophotometer and ^1H NMR spectra were recorded on Bruker Avance II 400 NMR Spectrometer using DMSO-d_6 and CDCl_3 as solvent and tetramethylsilane (TMS) as internal reference standard. Horse gram seeds (*Macrotyloma uniflorum*) were collected from departmental store, Hyderabad. Fourier transforms infrared spectroscopy (FTIR) study of the nanoparticles was performed on Shimadzu, Japan, using KBr as a reference.

Synthesis of Biginelli compounds compound **1** and compound **2** were synthesized following the literature method [15] and characterized using spectral analysis.



Compound 1



Compound 2

Synthesis of green Nano-Biginelli compounds

Biosynthesis of nanoparticles using plants or plant based extracts is safe and have relatively short production times as well as lower production cost compared to other biological systems. For the synthesis of green nanoparticles, Horse gram seeds extract is used. The first step in the

synthesis of green nanoparticles is the collection of black coated horse gram seeds (Figure 1a). The next step is the germination of seeds (Figure 1b) for which the seeds were washed with KMnO_4 solution. After washing, the seeds were soaked in distilled water for about 12 hours. The seeds were allowed to germinate and they were moistened with distilled water regularly for every 12 hours. The germinated seeds are freeze dried and are grounded to 60 mesh size in acetone. The mixture obtained was filtered through double layer whatmann filter paper number 1. The dry homogenate was coarsely ground using mortar and pestle and the powder was then suspended in the phosphate buffer solution. This mixture was further filtered and centrifuged at 10000 rpm for 8 min below 4°C and the supernatant collected contains enzyme, protease which was mixed with the synthesized Biginelli compounds compound 1 and compound 2. After 2-3 days, compounds were converted into nano particles.



Figure 1a. Horse gram seeds.



Figure 1b. Germinated seeds.

Characterization of Nano-Biginelli compounds

The newly synthesized nanoparticles were characterized by using UV-Visible spectra, FTIR (Fourier transform infrared spectroscopy), XRD (X-ray diffraction) and SEM (scanning electron microscopy).

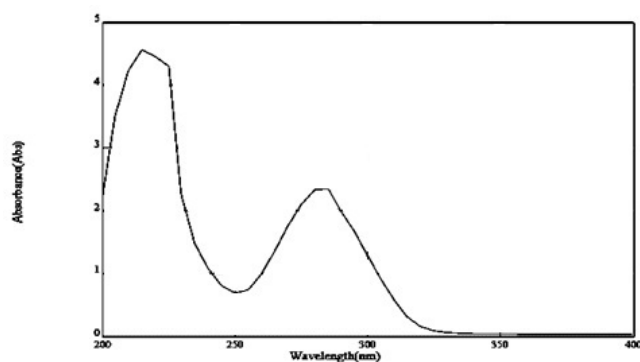


Figure 2. UV-Visible absorption spectra of compound 2 nanoparticles.

UV-Visible spectroscopy

UV-Visible absorption spectra of compound 2 nanoparticles (Figure 2) indicates that a band due to the $>\text{C}=\text{N}$ chromophore in the spectrum of the compound at 285 nm shifts to a higher wavelength. Such a shift in $n-\pi^*$ transition band is probably due to the donation of a lone pair

of electrons by the nitrogen. Further, two bands at 260 nm and 305 nm are due to π - π^* transitions which are assigned to the benzenoid ring and (NH) band of the pyrimidine ring respectively. The K band π - π^* showed a red shift due to the increase in conjugation and the B-band undergoes a hypsochromic shift.

Fourier transforms infrared spectroscopy

A 0.25 g dried sample (compound **2** nanoparticles) was mixed with KBr (sample/KBr ratio was 1/100) and pressed into the transparent thin pellet.

X-Ray powder diffraction of nanoparticles

Powder X-ray diffraction patterns of the prepared sample were taken by a two-circle (**2 θ - θ**), X-ray powder diffractometer (*X'Pert PRO XRD PW 3040 system*) using Copper ka_1 of wavelength 1.54056 Å and ka_2 of wavelength 1.544426 Å. The scan was taken between 2θ of 10° and 2θ of 71.89° at increments of 0.04° with a count time of 4 seconds for each step (Figure 3).

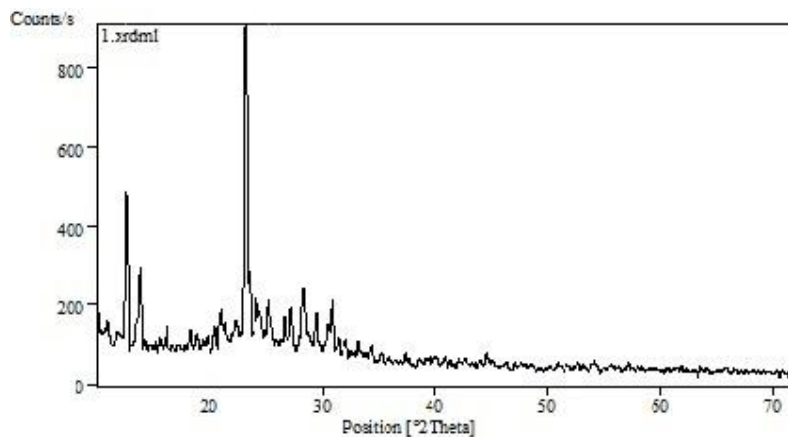


Figure 3. XRD pattern of compound **2** nanoparticles.

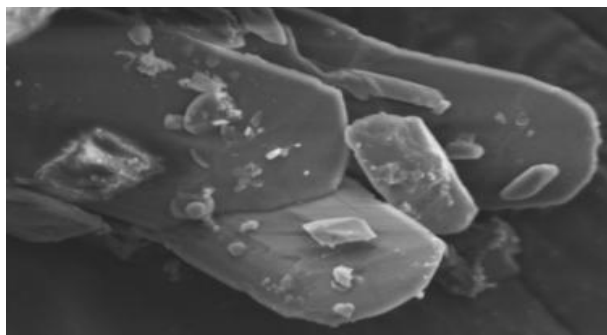


Figure 4a. SEM of compound **1** nanoparticles.

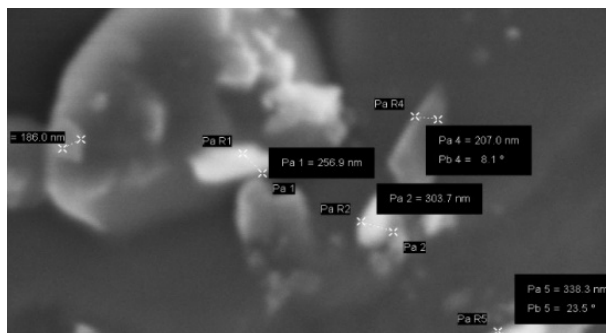


Figure 4b. SEM of compound **2** nanoparticles.

RESULTS AND DISCUSSION

Biginelli reaction is an important multicomponent reaction for the formation of Biginelli compounds. The classical Biginelli reactions were conducted under strongly acidic conditions, which suffer from various drawbacks like poor yields, long reaction times, and sensitive functional groups are lost during the reaction conditions. This has led to the development of several new methodologies, which improve the yields compared to the original procedure. These new strategies involve the use of following catalysts, e.g. $\text{BF}_3 \cdot \text{OEt}_2$, montmorillonite (KSF), polyphosphate esters and reagents like LiBr [16], TMSCl/NaI [17], $\text{LaCl}_3 \cdot 7\text{H}_2\text{O}$ [18], $\text{CeCl}_3 \cdot 7\text{H}_2\text{O}$ [19], $\text{Mn}(\text{OAc})_3 \cdot 2\text{H}_2\text{O}$ [20], FeCl_3 and HCl [21], ytterbium triflate [22], iodine [23], ZnCl_2 [24], CoCl_2 [25], etc. We have synthesized Biginelli compounds compound **1** and compound **2** using our reported literature method and converted these Biginelli compounds to Nano-Biginelli compounds with the help of enzyme extracted naturally from plants.

In recent years, plant mediated biological synthesis of nanoparticle is achieving significance due to its consistency and eco-friendliness [26]. Horse gram scientifically known as *Macrotyloma uniflorum* is widely consumed as staple diet in Southern parts of India. Other name variations of Horse gram are Kulthi bean, Madras gram, Hurali and Horse gram. It plays an important role in the inhibition/dissolution of calcium oxalate and gallbladder stone. Medicinal values and edibility of the pulse are already established [27]. Horse gram seed extracts contain enzyme protease which was mixed with the synthesized Biginelli compounds compound **1** and compound **2**. After 2-3 days, compounds were converted into nano particles. There is no report available in the literature regarding the synthesis of green Nano-Biginelli compounds. Further, the nanoparticles have also been characterized using UV, FTIR, XRD and SEM images and prediction of the anticancer potentiality of Biginelli nanoparticles is being carried out by molecular docking and ADMET techniques.

FTIR spectrum was obtained in the range 3242 to 781 cm^{-1} indicating peaks at 3242 cm^{-1} (m) for N-H stretch, 1722 cm^{-1} for C=O stretch, peaks at 1645 and 1600 cm^{-1} for C=C stretch in the aromatic compounds. A very weak peak at 1630 cm^{-1} is also observed for C=C aromatic stretch and peaks at 1462 , 1388 and 2980 cm^{-1} indicate the C-H bend in CH_3 and CH_2 , 1091 cm^{-1} for C-O-C of ethyl and pyrimidine ring and at 781 cm^{-1} is for C-Cl stretch.

The XRD spectrum of compound **2** nanoparticles in Figure 3 shows that there are two Bragg diffraction peaks at near $2\theta = 12.68^\circ$ and 23.17° . The present study, the peaks at near $2\theta = 12.68^\circ$ and 23.17° correspond to the presence of large amounts of amorphous compound **2** Nano-materials in association with cubic lattice system [28].

SEM images of compound **1** and compound **2** nanoparticles in the range 180-300 nm indicating the formation of nanoparticles (Figure 4).

Protein preparation

The human DNA topoisomerase I protein structure complexed with Camptothecin is retrieved from the PDB database (PDB ID: 1T8I) having a resolution of 3.0 Å and is imported into Accelrys Discovery Studio 2.1. Further using the clean protein protocol within Discovery Studio, the protein is prepared for correcting the lack of hydrogen atoms, missing atoms and residues, incorrect atom order in amino acids, to complete the protein chain. Water molecules are removed, and protonating all the residues at a pH of 7.4 is done thus allowing the protonation of arginine and lysine side chains and deprotonation of glutamate and aspartate side chains. The protonation of histidine side chains is selective in accordance with their context in the target. All the heteroatoms are removed except Camptothecin, which is used later for defining the binding site. To the entire protein complex of human DNA topoisomerase I and Camptothecin, CHARMM force field is applied for protein preparation with potential energy of -16901.16 kcal/mol, Van der Waals energy of -1848 kcal/mol and an initial RMS (root-meansquare) gradient energy of 0.2428 kcal/mol. By using smart minimizer algorithm with a maximum number of steps 1000 and RMS gradient 0.1, energy minimization is performed that carry forward using steepest descent and conjugate gradient algorithm till the protein complex (Figure 5).

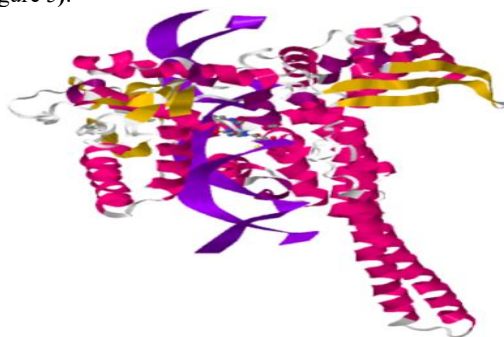


Figure 5. Human DNA Topoisomerase I (70 kda) in complex with the poison camptothecin.

Preparation of ligand dataset

The synthesized compounds compound **1** and compound **2** were drawn using ACD/ChemSketch (12.0), the two-dimensional structures of all the compounds are drawn and saved in mol file format, later imported in to discovery studio and energy minimization carried out through appliance of smart minimizer algorithm with a maximum number of steps 1000 and RMS gradient 0.1 which continues by steepest descent and conjugate gradient algorithm until the compounds are satisfied with a convergence gradient of 0.001 kcal mol⁻¹. Further diverse conformations for each ligand are generated using DS diverse conformation generation module which employs the Poling algorithm. A maximum of 255 conformations are created per compound using FAST conformer method in reach of an energy range 20 kcal/mol over the global energy minimum. This preferred maximal value of conformations ensures an adequate inclusion of conformational space. Default settings are kept for the other parameters.

Define binding site

After the protein complex is energy minimized, by using Define and Edit Binding Site tools in Accelrys Discovery Studio 2.1 the binding site of the human DNA topoisomerase I is predicted. The protein binding site was determined based on the occupied volume of the

known ligand Camptothecin in the active site. The co-crystallized Camptothecin molecule is first selected, and a sphere is created around the molecule using define sphere from the selection option. A sphere is defined around the residues comprising binding site at a radius of 10 Å.

Molecular docking studies (docking strategy)

For accurate docking of our synthesized compounds into active site of the protein, molecular docking is carried out through LibDock module in Accelrys Discovery Studio 2.1. LibDock is a high-throughput site-featured docking algorithm. The binding site features are called as 'hotspots' in which these site spheres are resolved with a grid fixed in active site. It counts the hotspot map for polar and apolar cluster in the active site of the protein which is further used for the alignment of the ligand conformations to the interaction sites of the protein for the formation of considerable interaction. Finally, it returns all the minimized ligand poses and their rankings based on the ligands score. In accordance with the LibDock score, each pose is assessed which uses a simple pair-wise method. For estimating binding energies of the protein–ligand complex, the ligands with high LibDock scores are preferred. The complex pose with the best binding energy is used for further binding mode analysis. For the docking validation, the co-crystallized ligand Camptothecin in the human DNA topoisomerase I binding site is redocked. The binding affinities of the synthetic compounds were compared and analyzed in reference to Camptothecin to identify structural characteristics of the complexes formed by these compounds and the protein.

ADMET studies

ADMET (absorption, distribution, metabolism, excretion and toxicity) analysis is done using Accelrys Discovery Studio 2.1 which accommodates the awareness of the pharmacokinetic properties of the synthesized compounds. ADMET properties include absorption, blood–brain barrier (BBB), aqueous solubility, hepatotoxicity, plasma protein binding (PPB) and cytochrome [29, 30].

Docking studies

To study the binding modes and affinities of our synthesized compounds with human DNA topoisomerase I (PDB ID: 1T8I), docking studies are carried out using LibDock. The best ligand conformation is selected on the basis of LibDock score and highly interacting amino acid residues. Of the ten conformations generated for each compound, compound **2** with the highest LibDock score is taken for interaction analysis of the hydrogen bonding. LibDock scores of all the compounds along with their hydrogen bond interactions and bond lengths are depicted in Table 1. From the overall docking and interaction analysis, the best conformation of the compound **2** docked complex shows high LibDock score of 134 kcal/mol and forms three hydrogen bonds with the protein human DNA topo I. Figure 6a depicts the hydrogen bond interactions of the enzyme human DNA topo I with the compound **2**. Hydrogen bonds are formed between the N14 of compound **2** interacting with the oxygen atom of the OP1:D G12 (compound **2** : N14 - C:DG12:OP1) with a hydrogen bond distance of 2.793 Å, two hydrogen bonds formed in between Thr718 with N13 of compound **2** with distance 2.650 Å and 2.051 Å. Another hydrogen bond formed with NH₂ of Arg 364 with O18 of compound **2** with a distance of 3.038 Å [31].

The hydrogen bond formations are represented in green-dotted lines and compound **2** is represented in ball-stick manner. The hydrogen bond formations are represented in green-dotted lines and compound **1** is represented in ball-stick view (Figure 6b).

Table 1. Docking scores of the compounds.

Compound	Libdock score	Interacting residues	Interacting residues	H-Distance
Compound 1	123.045	ARG364 THR718 TGP11 DT10 Asp722 DG12 DC112 DA113 Asp533	A:ARG364:HH22- Compound 05:O19 A:THR718:HG1 – Compound 05:N14 Compound 05:H30 - A:THR718:OG1 Compound 05:H31 - A:THR718:OG1 Compound 05:H32 - C:TGP11:O4'	2.051000 2.121000 2.169000 1.949000 1.344000
Compound 2	134.284	ARG364 THR718 TGP11 DT10 Asp722 DG12 DC112 DA113 Asp533	Compound 06:N14 - C:DG12:OP1 A:ARG364:NH2 – Compound 06:O18 Compound 06:N13 - A:THR718:OG1 Compound 06:N13 - A:THR718:OG1	2.793000 3.038000 2.650000 2.051000

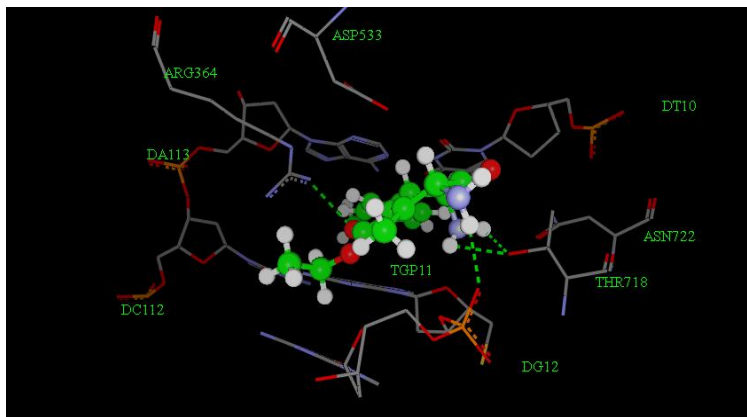


Figure 6a. Hydrogen bond interactions of a compound 2 with human DNA topo I (PDB ID:1T8I).

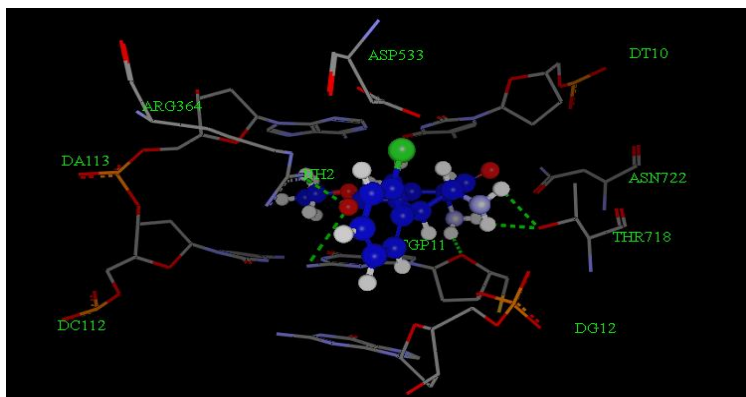


Figure 6b. Hydrogen bond interactions of a compound compound **1** with human DNA topo I (PDB ID:1T8I).

ADMET results

The compounds are further examined for their pharmacokinetic and toxicity studies using ADMET descriptors analysis protocol in Discovery Studio [32]. Using the standards provided by Discovery Studio, the results are analyzed. The calculated parameters are tabulated in Table 2. According to the Discovery Studio parameters, standard analysis value like level 0 for human intestinal absorption, level 3 and level 4 for solubility, level 0 for non-inhibitory property with CYP450 2D6, level 3 for BBB penetration and level 0 for non-toxicity was filtered for obtaining drug-like compounds. BBB penetration and level 0 for non-toxicity was filtered for obtaining drug-like compounds. Figure 7 shows the plot of predicted values of drug absorption for our compounds. ADMET descriptors, the 2D polar surface area (PSA_{2D}) in Å² per compound is plotted against their consonant estimated atom-type partition coefficient (ALogP98).

Table 2. Absorption, distribution, metabolism, excretion and toxicity.

Compound	ADMET_BB B Level	ADMET_Abs orption Level	ADMET_Solub ility Level	ADMET_Hepato toxicity	ADMET_C YP2D6
Compound 1	3	0	2	0	0
Compound 2	3	0	3	1	0

Finally, the ADMET studies deal with *in silico* prediction of the adverse effects of the synthesized compounds. These properties such as absorption, distribution, metabolism, excretion and toxicity (ADMET) are important in order to determine the success of the compound for human therapeutic use. The results were compared to the reference level values of Discovery Studio to analyze the properties of our compounds. The absorption levels (human intestinal absorption) of both the compounds are predicted to be having good absorption. Intestinal absorption is defined as a percentage absorbed rather than as the ratio of concentrations. The solubility levels of the compounds were in the range of 2–3, indicating good solubility for the compounds having the value 3 and less soluble for the compounds having the value 2. Both the compounds exhibited *in silico* cytochrome p4502D6 inhibition. Similarly, both the compounds are satisfactory with respect to CYP2D6 value as 0, suggesting that these compounds should be non-inhibitors of CYP2D6. In principle, cytochrome p4502D6 is involved in the metabolism of a variety of substrates in the liver and its inhibition

by a drug constitutes major cases of drug–drug interactions. The partial plasma binding ability of the compounds influences the efficacy of the drug, since the bound fraction is temporarily shielded from metabolism and only the unbound fraction exhibits pharmacological effects. Finally, the plasma protein binding property prediction denotes that both of them have binding C95% indicating that compounds have good bioavailability and are not likely to be highly bound to carrier proteins in the blood. Further, both the compounds have been predicted to have the probability hepatotoxicity levels less than 1.

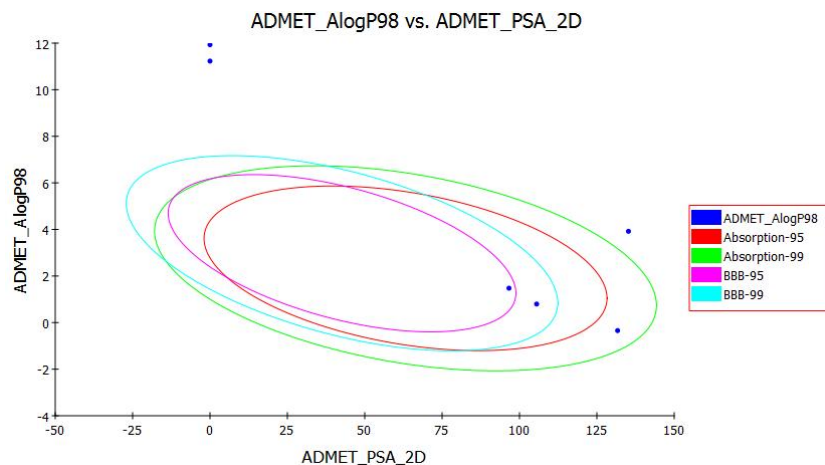


Figure 7. Plot of PSA versus log P for candidate compounds showing the 95 and 99% confidence limit; ellipses corresponding to the blood–brain barrier and intestinal absorption models.

CONCLUSION

Biological green synthesis of novel Biginelli-Nanoparticles is successfully achieved which is one of the environment-friendly green chemistry based techniques. ADMET studies indicate that absorption levels (human intestinal absorption) of both the compounds are predicted to be having good absorption. Both the compounds exhibited in silico cytochrome p4502D6 inhibition. Similarly, both the compounds are satisfactory with respect to CYP2D6 value as zero, suggesting that these compounds should be non-inhibitors of CYP2D6. Combining the results of molecular docking, pharmacophore and ADMET studies, we have found that the compound **1** (ethyl-6-methyl-2-oxo-4-(4-methoxyphenyl)-1,2,3,4-tetrahydropyrimidin-5-carboxylate) has all qualities to leads as a newest human Aurora B kinase inhibitor.

ACKNOWLEDGEMENTS

The authors are thankful to the SAIF, Punjab University, Chandigarh for carrying out the spectral and elemental analyses of the synthesized compounds.

REFERENCES

1. Shah, M.; Fawcett, D.; Sharma, S.; Tripathy, S.; Poinern, G. Green synthesis of metallic nanoparticles via biological entities. *Materials* **2015**, *8*, 7278-7308.

2. Kidwai, M.; Bansal, V.; Saxena, A.; Aerry, S.; Mozumdarb, S. Cu-Nanoparticles: Efficient catalysts for the oxidative cyclization of Schiff's bases. *Tetrahedron Lett.* **2006**, 47, 8049-8053.
3. Dandia, A.; Parewa, V.; Jain, A.K.; Rathore, K.S. Step-economic, efficient, ZnS nanoparticle-catalyzed synthesis of Spiro oxindole derivatives in aqueous medium via Knoevenagel condensation followed by Michael addition. *Green Chem.* **2011**, 13, 2135-2145.
4. Varasteh, M.A. ZnO-nanoparticles as an efficient catalyst for the synthesis of tetrasubstituted cyclopentadienones using sulfonoketenimides and enaminoesters. *Phosphorus Sulfur Silicon Relat. Elem.* **2018**, 193, 45-49.
5. Sachdeva, H.; Saroj, R. ZnO nanoparticles as an efficient, heterogeneous, reusable, and ecofriendly catalyst for four-component one-pot green synthesis of pyranopyrazole derivatives in water. *Sci. World J.* **2013**, 2013, Article ID 680671.
6. Ghosh, B.K.; Ghosh, N.N. Applications of metal nanoparticles as catalysts in cleaning dyes containing industrial effluents: A review. *J. Nanosci. Nanotechnol.* **2018**, 18, 3735-3758.
7. Huang, Z.; Chen, Z.; Chen, Z.; Lv, C.; Meng, H.; Zhang, C. Ni12P5 nanoparticles as an efficient catalyst for hydrogen generation via electrolysis and photoelectrolysis. *ACS Nano* **2014**, 8, 8121-8129.
8. Ahmad, A.; Senapati, S.; Khan, M.I.; Kumar, R.; Sastry, M. Extracellular biosynthesis of monodisperse gold nanoparticles by a novel extremophilic actinomycete thermomonospora sp. *Langmuir* **2003**, 19, 3550-3553.
9. Roh, Y.; Lauf, R.J.; McMillan, A.D.; Zhang, C.; Rawn, C.J.; Bai, J.; Phelps, T.J. Microbial synthesis and the characterization of metal-substituted magnetites. *Solid State Commun.* **2001**, 118, 529-534.
10. Mukherjee, P.; Ahmad, A.; Mandal, D.; Senapati, S.; Sainkar, S.R.; Khan, M.I.; Parishcha, R.; Aiayumar, P.V.; Alam, M.; Kumar, R. Fungus-mediated synthesis of silver nanoparticles and their immobilization in the mycelia matrix: A novel biological approach to nanoparticles synthesis. *Nano Lett.* **2001**, 1, 515-519.
11. Lee, S.W.; Mao, C.; Flynn, C.; Belcher, A.M. Ordering of quantum dots using genetically engineered viruses. *Science* **2002**, 296, 892-895.
12. Philip, D. Green synthesis of gold and silver nanoparticles using *Hibiscus rosa sinensis*. *Physica E* **2010**, 42, 1417-1424.
13. Vidhu, V.K.; Aromal, S.A.; Philip, D. Green synthesis of silver nanoparticles using *Macrotyloma uniflorum*. *Spectrochim. Acta A* **2011**, 83, 392-397.
14. Fátima, Á.de.; Braga, T.C.; Neto, L.D.S.; Terra, B.S.; Oliveira, B.G.; da Silva, D.L.; Modolo, L.V. A mini-review on Biginelli adducts with notable pharmacological properties. *J. Adv. Res.* **2015**, 6, 363-373.
15. Sachdeva, H.; Dwivedi, D. Lithium-acetate-mediated biginelli one-pot multicomponent synthesis under solvent-free conditions and cytotoxic activity against the human lung cancer cell line A549 and breast cancer cell line MCF7. *Sci. World J.* **2012**, 2012, Article ID 109432.
16. Baruah, P.P.; Gadhwal, S.; Prajapati, D.; Sandhu, J.S. The Biginelli condensation: A novel and efficient regioselective synthesis of dihydropyrimidin-2(1H)-ones using lithium bromide. *Chem. Lett.* **2002**, 31, 1038-1039.
17. Zhu, Y.; Pan, Y.; Huang, S. Trimethylsilyl chloride: A facile and efficient reagent for one-pot synthesis of 3, 4-dihydropyrimidin-2(1H)-ones. *Synth. Commun.* **2004**, 34, 3167-3174.
18. Lu, J.; Bai, Y.; Wang, Z.; Yang, B.; Ma, H. One-pot synthesis of 3,4-dihydropyrimidin-2(1H)-ones using lanthanum chloride as a catalyst. *Tetrahedron Lett.* **2000**, 41, 9075-9078.
19. Bose, D.S.; Fatima, L.; Mereyala, H.B. Green chemistry approaches to the synthesis of 5-alkoxycarbonyl-4-aryl-3,4-dihydropyrimidin-2(1H)-ones by a three-component coupling of

- one-pot condensation reaction: Comparison of ethanol, water, and solvent-free conditions. *J. Org. Chem.* **2003**, 68, 587-590.
20. Kumar, K.A.; Kasthuraiah, M.; Reddy, C.S.; Reddy, C.D. Mn(OAc)₃·2H₂O-mediated three-component, one-pot, condensation reaction: an efficient synthesis of 4-aryl-substituted 3,4-dihydropyrimidin-2-ones. *Tetrahedron Lett.* **2001**, 42, 7873-7875.
 21. Zorkun, İ.S.; Saraç, S.; Çelebi, S.; Erol, K. Synthesis of 4-aryl-3,4-dihydropyrimidin-2(1H)-thione derivatives as potential calcium channel blockers. *Bioorg. Med. Chem.* **2006**, 14, 8582-8589.
 22. Pittayakhajonwut, P.; Suvannakad, R.; Thienhirun, S.; Prabpai, S.; Kongsaree, P.; Tanticharoen, M. An anti-herpes simplex virus-type 1 agent from *Xylaria mellisii* (BCC 1005). *Tetrahedron Lett.* **2005**, 46, 1341-1344.
 23. Srinivas, K.V.N.S.; Das, B. Iodine catalyzed one-pot synthesis of 3,4-dihydropyrimidin-2(1H)-ones and thiones: A simple and efficient procedure for the Biginelli reaction. *Synthesis* **2004**, 2004, 2091-2093.
 24. Jagwani, D.; Joshi, P. A greener chemistry approach for synthesis of 4-(4-hydroxyphenyl)-6-methyl-2-oxo-1,2,3,4-tetrahydropyrimidine-5-carboxylic acid ethyl ester, *Int. J. Pharm. Sci. Res.* **2015**, 6, 783-790.
 25. Lu, J.; Bai, Y.J.; Guo, Y.H.; Wang, Z.J.; Ma, H.R. CoCl₂·6H₂O or LaCl₃·7H₂O catalyzed Biginelli reaction. One-pot synthesis of 3,4-dihydropyrimidin-2(1H)-ones. *Chin. J. Chem.* **2002**, 20, 681-687.
 26. Vichai, V.; Kirtikara, K. Sulforhodamine B colorimetric assay for cytotoxicity screening. *Nat. Protoc.* **2006**, 1, 1112-1116.
 27. Dangi, B.; Kaul, V.K.; Kothari, S.L.; Kachhwaha, S. Micropropagation of *Terminalia bellerica* from nodal explants of mature tree and assessment of genetic fidelity using ISSR and RAPD markers. *Physiol. Mol. Biol. Plants* **2014**, 20, 509-516.
 28. Cullity, B.D.; Stock, S.R. *Elements of X-Ray Diffraction*, 3rd ed., Prentice Hall: Upper Saddle River; New Jersey; **2001**.
 29. Fuller, D.Q.; Murphy, C. The origins and early dispersal of horsegram (*Macrotyloma uniflorum*), a major crop of ancient India. *Genet. Resour. Crop Evol.* **2018**, 65, 285-305.
 30. Venkanna, A.; Siva, B.; Poornima, B.; Vadaparathi, P.R.; Prasad, K.R.; Reddy, K.A.; Reddy, G.B.; Babu, K.S. Phytochemical investigation of sesquiterpenes from the fruits of *Schisandra chinensis* and their cytotoxic activity. *Fitoterapia* **2014**, 95, 102-108.
 31. Baby, S.T.; Sharma, S.; Enaganti, S.; Cherian, R.P. Molecular docking and pharmacophore of heterocyclic compounds as heat shock protein 90 (Hsp90) inhibitors. *Bioinformation* **2016**, 12, 149-155.
 32. Vadlakonda, R.; Nerella, R.; Enaganti, S. Theoretical studies on azaindoles as human aurora B kinase inhibitors: Docking, pharmacophore and ADMET studies. *Interdiscip. Sci. Comput. Life Sci.* **2016**, 10, 1-14.